Electronic Supplementary Material (ESI) for RSC Advances.

Supporting Information

Effect of pre-shear on structural behavior and pipeline restart of gelled waxy crude oil

Youquan Bao, Jinjun Zhang*, XinyiWang, Wenwen Liu

National Engineering Laboratory for Pipeline Safety/ MOE Key Laboratory of Petroleum Engineering/ Beijing Key Laboratory of Urban Oil & Gas Distribution Technology, China University of Petroleum-Beijing, Beijing 102249, China

* Corresponding author. Tel: +86-10-8973-4627; Fax: +86-10-8973-4627.

E-mail address: zhangjj@cup.edu.cn

1. Repeatability tests of SAOS and stepwise increases in shear rate

Fig. S1 and Fig. S2 show the repeatability tests of SAOS and stepwise increases in shear rate. It is obvious that the repeatability is good.

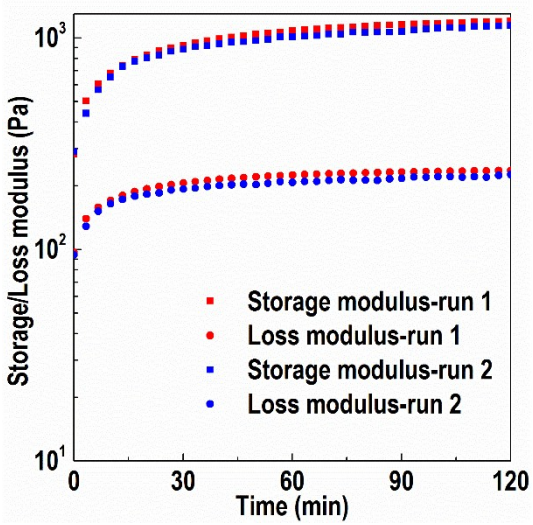

Fig. S1. Repeatability test of SAOS (pre-shear temperature $T_{p\text{-}s}$=34 °C and rate of pre-shear $\dot{\gamma}_{p\text{-}s}$ =0 s^{-1})

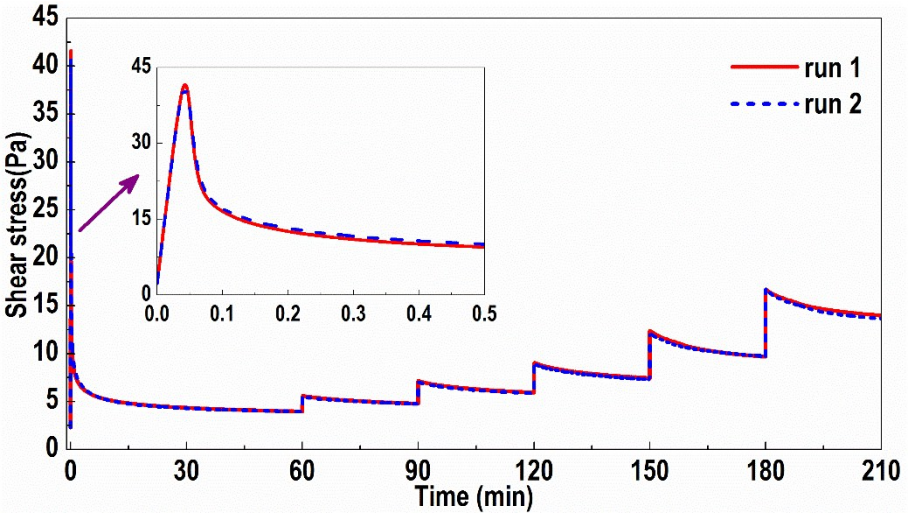

Fig. S2. Repeatability test of stepwise increases in shear rate (pre-shear temperature $T_{p\text{-}s}$=34 °C and rate of pre-shear $\dot{\gamma}_{p\text{-}s}$ =0 s^{-1})

2. Comparison between test results and fitted results of shear stress responses to stepwise increases in shear rate

Fig. S3 shows the comparison between the test results and fitted results of shear stress responses to stepwise increases in shear rate for different pre-shear conditions. It can be seen that the overlap between test results and fitted results is good.

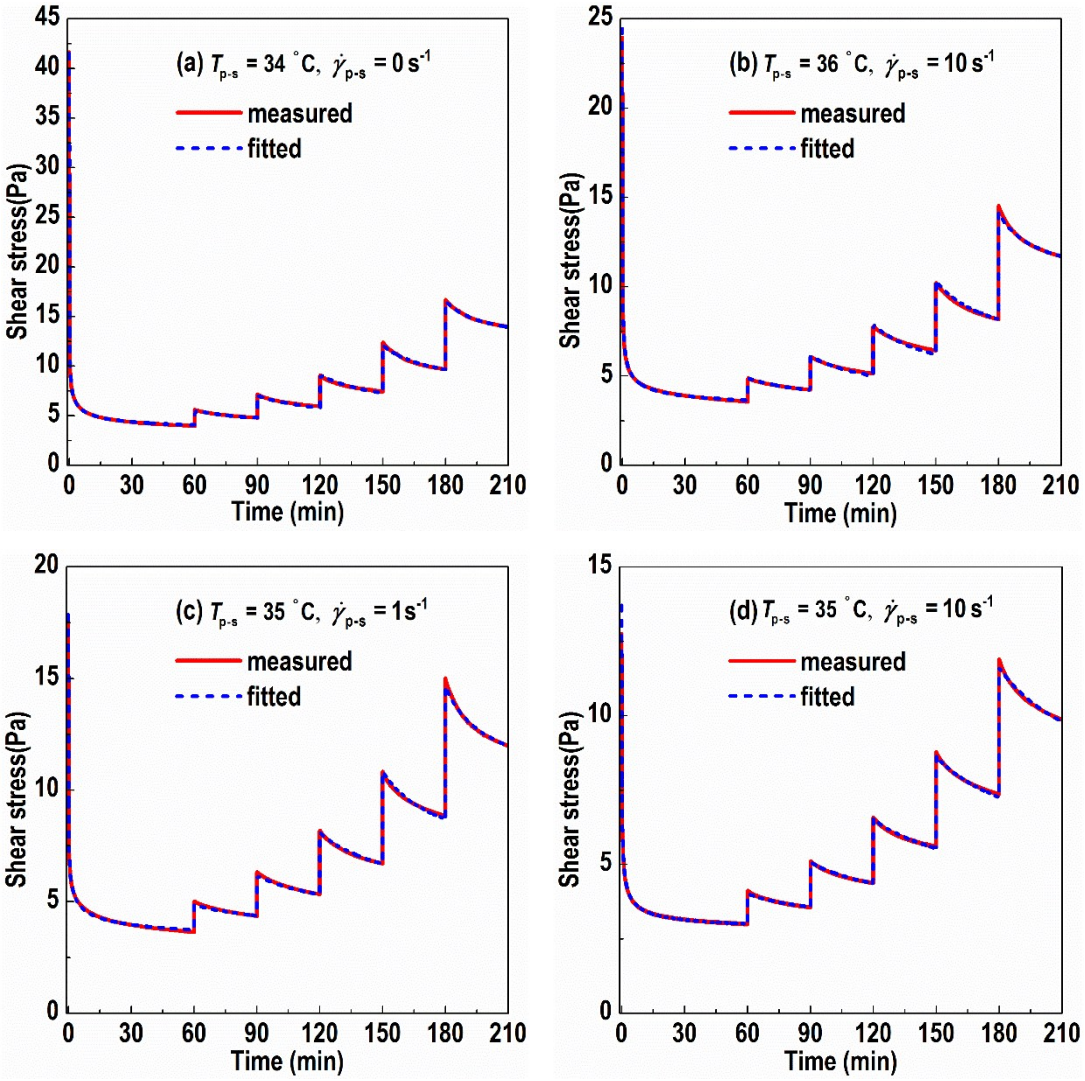

Fig. S3. Comparison between test results and fitted results of shear stress responses to stepwise increases in shear rate

3. Mesh size study

To ensure the mesh independence of the simulation results, the effect of mesh size on the simulation results is investigated. Five combinations of grid numbers are shown in Table S1, and the condition of $T_{p\text{-}s}$=35 °C, $\dot{\gamma}_{p\text{-}s}$=10 s^{-1} and P_{in}^{*}=0.003 is taken as an example to show the results of the mesh size study.

Fig. S4 shows the radial distribution of the inlet velocity for different radial mesh sizes at times t^{*}=1 and t^{*}=10. The results for radial grid numbers N_r=25 and N_r=50 are almost the same, so the radial grid number is conservatively set to 50. Fig. S5 shows the time evolution of pressure P^{*} at axial positions z^{*}=1 and z^{*}=0.9 for different axial mesh sizes. There are some high-frequency oscillations around time t^{*}=1 if the grid is sparse, and the oscillation amplitude

decreases with increasing axial grid number. When the number of axial grids is equal to or greater than 300, the oscillation disappears, so the axial grid number N_z=500 is conservatively confirmed.

Table S1. Combinations of grid number in axial direction and radial direction

Mesh	N_z	N_r
Mesh 1	500	10
Mesh 2	500	25
Mesh 3	500	50
Mesh 4	300	50
Mesh 5	100	50

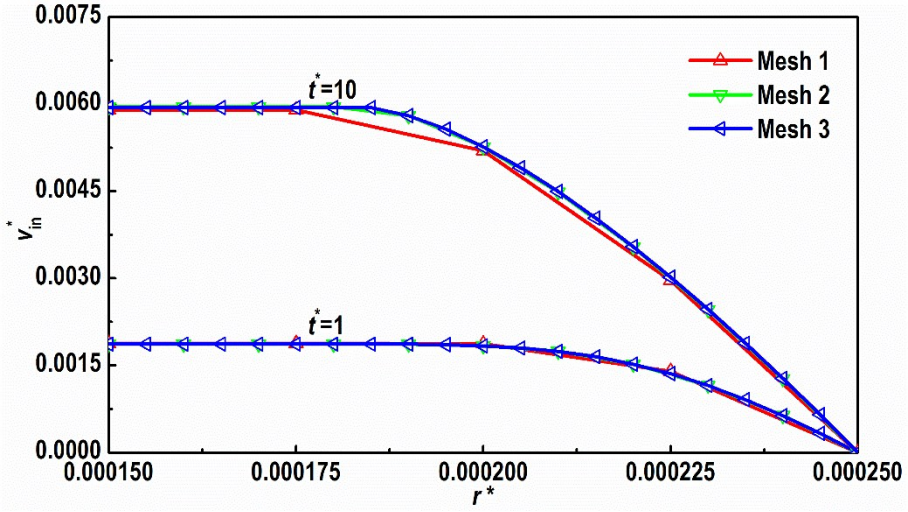

Fig. S4. Radial distribution of inlet velocity for different radial mesh sizes

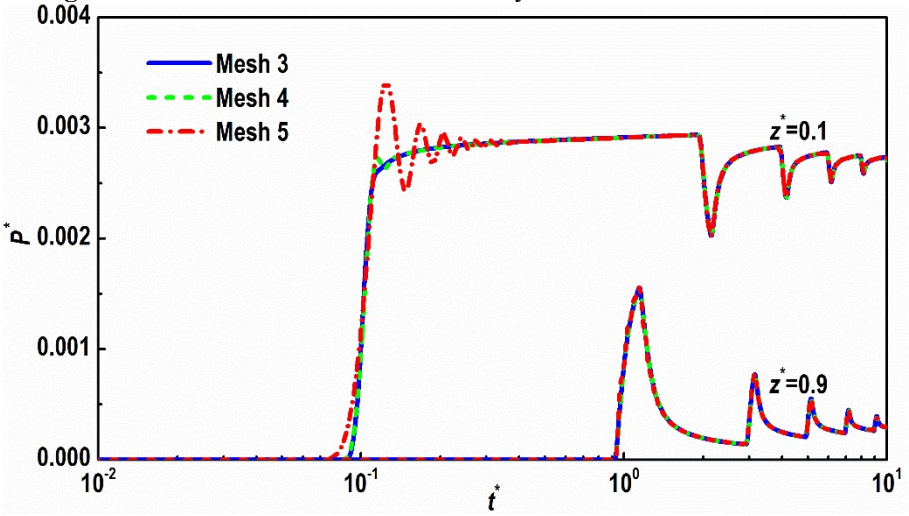

Fig. S5. Time evolution of pressure at the axial positions z^*=1 and z^*=0.9 for different axial mesh sizes